IVB imido complexes. Further evidence for the potential importance of this interaction in stabilizing the TS versus reactants was found in the IRC; the MH$_1$ distance is at a minimum when H$_t$ is midway between C and N, presumably the point at which it has the greatest need of a bonding interaction. The MH$_1$ interaction is one-quarter of that in a normal metal–terminal hydride bond, as measured by the BOP. Low-energy, vacant d oribtals on the metal seem a likely source for interaction with H$_1$. Consistent with this proposal is the much higher barrier for 1,2-methane elimination in $(H)_2Si(CH_3)(NH_2)$ (83.3 kcal mol^{-1}), in which d orbital participation will be less or nonexistant.[43] It is tempting to infer that the design of catalyst and material precursors ($L_nM(X)E(H_1)$) which enhance the MH$_1$ interaction will lower barriers to alkane activation and elimination and lead to catalysts which are more active and CVD precursors which can be processed at lower temperatures. Studies are in progress[43] to assess the effect on the MH$_1$ interaction (and its correlation to barrier heights) which results from modification of the leaving group (X), metal (M), and ligand (E).

Acknowledgment. The author wishes to thank Mark Gordon, Mike Schmidt, and the rest of the Iowa State Quantum Chemistry Group for providing us with the latest copy of GAMESS and helpful discussions. Helpful discussions and the communication of unpublished results by Peter T. Wolczanski (Department of Chemistry, Cornell University) and Jan H. Jensen (Department of Chemistry, Iowa State University) are also gratefully acknowledged. A grant to T.R.C. of time on the Cray Y-MP8/864 (Grant No. CHE920007N) at the National Center for Supercomputing Applications (NCSA), administered by the National Science Foundation, was instrumental in carrying out several of the larger calculations reported here. The bulk of the calculations described here were carried out at MSU on a DECstation 5000/200, which was a generous loan of the Digital Equipment Corporation. Additional funding was provided by the Department of Chemistry and Memphis State University (through a Faculty Research Grant).

---

[43] Cundari, T. R.; Gordon, M. S. *J. Am. Chem. Soc.* Submitted for publication.

Incorporation of Hydration Effects within the Semiempirical Molecular Orbital Framework. AM1 and MNDO Results for Neutral Molecules, Cations, Anions, and Reacting Systems

George P. Ford* and Bingze Wang

Contribution from the Department of Chemistry, Southern Methodist University,
Dallas, Texas 75275. *Received May 29, 1992*

Abstract: A recently developed continuum model for the incorporation of hydration effects into the AM1 and MNDO semiempirical molecular orbital Hamiltonians is evaluated by comparison with representative experimental data. The new method gives quantitatively correct predictions for the aqueous-phase conformational behavior of $H_3N^+CH_2CH_2CO_2^-$ and the aqueous-phase activation energetics of the S_N2 reaction of Cl^- and CH_3Cl. The dissociation energetics of *t*-BuCl are correctly predicted, while the computed dissociation pathway includes a shallow energetic minimum corresponding to the expected tight ion pair. The absolute hydration energies of neutral molecules and cationic and anionic species are generally predicted satisfactorily. Systematic deviations from the experimental data due to the intervention of hydrophobic effects (not currently allowed for) as well as those traceable to the simplified integral treatment are noted. Contrary to intuition, continuum methods apparently can give quantitatively reliable hydration energies for species in which specific hydrogen-bonding effects are generally considered to be important. This was true for protonated amines, although only partially so for protonated oxygen bases.

Introduction

The reaction field approach has attracted much recent attention as a general basis for the computation of solvation energies.[1,2] Despite the crudeness of the model, in which the solvent is treated as a structureless dielectric continuum, it appears to offer considerable promise in chemical, biochemical, and pharmacological applications. To date, development of the theory within the quantum mechanical framework has evolved in three distinct directions. In one, the solute is placed in an ellipsoidal or often simply a spherical cavity within the solvent with which it interacts via its dipole or in some cases higher-order multipole moments.[3–5] Although this method has enjoyed considerable popularity, there are obvious limitations associated with the need to constrain an arbitrarily shaped solute to a cavity of specified shape. For similar reasons, its application to reaction processes is highly limited.

In the so-called extended Born approach, the solute is treated as an array of atom-centered spheres, each of which contributes to the overall hydration energy in a manner related to Born's original treatment of monatomic ions.[6–12] A number of appli-

---

[1] Tapia, O. In *Quantum Theory of Chemical Reactions*; Daudel, R., Pullman, A., Salem, L., Veillard, A., Eds.; Reidel: Dortrechi, 1980; Vol. 2, pp 25–72. Tapia, O. *Molecular Interactions*; Ratajczak, H., Orville-Thomas, W. J., Eds.; Wiley: New York, 1982; Vol. 3, pp 47–117.

[2] Drummond, M. L. J. *Prog. Biophys. Molec. Biol.* **1986**, *47*, 1–29.

[3] McCreery, J. H.; Christoffersen, R. E.; Hall, G. G. *J. Am. Chem. Soc.* **1976**, *98*, 7191–7197.

[4] Rinaldi, D.; Ruiz-Lopez, M. F.; Rivail, J.-L. *J. Chem. Phys.* **1983**, *78*, 834–838.

[5] Karelson, M. M.; Tamm, T.; Katritzky, A. R.; Cato, S. J.; Zerner, M. C. *Tetrahedron Comput. Methodol.* **1989**, *2*, 295–304. Katritzky, A. R.; Karelson, M. *J. Am. Chem. Soc.* **1991**, *113*, 1561–1566.

[6] Klopman, G. *Chem. Phys. Lett.* **1967**, *1*, 200–202.

[7] Germer, H. A., Jr. *Theor. Chim. Acta* **1974**, *34*, 145–155; *35*, 273–274.

[8] Constanciel, R.; Contreras, R. *Theor. Chim. Acta* **1984**, *65*, 1–11.

[9] Kozaki, T.; Morihashi, K.; Kikuchi, O. *J. Mol. Struct.* (*THEOCHEM*) **1988**, *168*, 265–277.

[10] Kozaki, T.; Morihashi, K.; Kikuchi, O. *J. Am. Chem. Soc.* **1989**, *111*, 1547–1552.

[11] Tucker, S. C.; Truhlar, D. G. *Chem. Phys. Lett.* **1989**, *157*, 164–170.

[12] Cramer, C. J.; Truhlar, D. G. *Science* **1992**, *256*, 231–217. Cramer, C. J.; Truhlar, D. G. *J. Am. Chem. Soc.* **1991**, *113*, 8552–8554, 8305–8311.

0002-7863/92/1514-10563$03.00/0

cations of this approach have appeared, including highly parameterized but promising versions within the AM1[12,13] and more recently within the PM3[13,14] frameworks by Cramer and Truhlar. Unfortunately, since the method lacks a clear physical basis,[2] interpretation of specific discrepancies between computed and experimental hydration energies is not straightforward, especially in view of the extensive parameterization involved.

In a third approach pioneered by Miertuš, Scrocco, and Tomasi,[15] the solute is placed in a cavity of arbitrary shape composed of finite surface elements. The reaction field is modeled by an induced charge on the cavity surface that is computed explicitly from the normal component of the electric field obtained from the molecular wave function. Various applications and refinements of this general procedure have been presented by the original workers[16-19] and others.[20]

Starting with many of the same ideas, we have developed a new formulation of this approach[21] which has been implemented in the semiempirical MOPAC package[22] using the AM1[23,24] and MNDO[25] Hamiltonians. Despite the fact that the current implementation is a rather simplified one, especially with respect to the cavity definition and the integral treatment, its ability to qualitatively and in most cases quantitatively predict the absolute hydration energies of organic molecules and ions, as well as account for the effects of the aqueous environment on reaction processes of diverse types, is surprisingly complete. This is particularly true in view of the fact that the method includes no parametric quantities beyond those that comprise the AM1 and MNDO methods. A full description of the method itself is given elsewhere.[21] The present paper focuses on its performance in the areas just mentioned.

Method

The solute is enclosed within an arbitrarily shaped cavity built from a system of overlapping atom-centered spheres. Those parts of the surface exposed to the solvent are divided into n surface elements, of which ca. 87% are hexagonal in shape and the remainder are pentagonal. Together they define the cavity surface which encloses the solute which is immersed in a continuous medium of dielectric constant ϵ. Polarization of the medium by the solute results in an electric field (the reaction field) which then acts back on the solute. In this model, the reaction field is represented by a set of n induced point charges Q_i associated with the n surface elements. The total Coulombic interaction between the surface charges and the electrons and nuclei of the solute is V_σ, which enters the relevant Schrödinger equation for a solute in a continuous dielectric shown in eq 1. $\hat{H}_{\mathrm{M}}$ and Ψ_{M} are the Hamiltonian and wave functions for the solute under the electrostatic perturbation of the medium.[26] The corresponding hydration energy is then the difference between the resulting total energy E_1 and that for the unperturbed solute molecule (eq 2). E_{t} can be expanded as shown in eq 3 in terms of the well-known electrostatic potential (eq 4). $V_{i_{\mu\nu}}$ describes the interaction between the charge associated with the ith surface element and the overlap distribution $\phi_\mu\phi_\nu$ and is closely analogous to the semiempirical core-electron attraction integral.[25] This formalism is used here, except the modifications of the classical multipole expression used in AM1 and MNDO to give the proper one-center behavior and correlation-related reductions of their magnitudes (which are not relevant here) are excluded. Further, for reasons related to the requirement that the overall charge on the cavity surface not deviate from the theoretical value,[21] we currently include only monopole components of the overlap distribution $\phi_\mu\phi_\nu$. With these simplifications, $V_{i_{\mu\nu}}$ reduces to the expression shown in eq 5, where $R_{\mathrm{A}i}$ is the distance form the ith surface element to nucleus A on which orbitals μ and ν are located.

$$(\hat{H}_{\mathrm{M}} + \tfrac{1}{2}V_\sigma)\Psi_{\mathrm{M}} = E_{\mathrm{t}}\Psi_{\mathrm{M}} \tag{1}$$

$$\Delta E_{\mathrm{solv}} = E_1(\Psi_{\mathrm{M}}) - E^0{}_1(\Psi^0{}_{\mathrm{M}}) \tag{2}$$

$$E_1(\Psi_{\mathrm{M}}) = E^0{}_1(\Psi_{\mathrm{M}}) + \tfrac{1}{2}\sum_i^n Q_iU_i \tag{3}$$

$$U_i = \sum_{\mu\nu} P_{\mu\nu}V_{i_{\mu\nu}} + \sum_A \frac{Z_A}{|s_i - R_A|} \tag{4}$$

$$V_{i_{\mu\nu}} = -\delta_{\mu\nu}/R_{\mathrm{A}i} \tag{5}$$

The Fock matrix for the solute in the presence of the solvent differs from that in the gas phase ($F^{\circ}{}_{\mu\nu}$) through the appearance of a summation over the surface elements (eq 6). The vector

$$F_{\mu\nu} = F^0{}_{\mu\nu} + \tfrac{1}{2}\sum_i^n [Q_iV_{i_{\mu\nu}} + U_i\,\partial Q_i/\partial P_{\mu\nu}] \tag{6}$$

of surface charges $\mathbb{Q}$ is obtained by solving the matrix equation

$$\mathbb{Q} = \mathcal{B}^{-1}\mathbb{Q}^0 \tag{7}$$

where

$$Q^0{}_i = -f_\epsilon \Delta s_i E_{i_{n,\rho}} \tag{8}$$

$$b_{ii} = 1 - 2\pi f_\epsilon(1 - (\Delta s_i/S_I)^{1/2}) \tag{9}$$

$$b_{ij} = f_\epsilon \Delta s_i \frac{\cos \alpha_{ij}}{|s_i - s_j|^2} \tag{10}$$

and $f_\epsilon = (\epsilon - 1)/4\pi\epsilon$. Δs_i is the area of surface element i, and S_I is the total surface area of the sphere on which it resides. $E_{i_{n,\rho}}$ is the normal component of the electric field through the surface element i due to the solute (designated by the suffix ρ). The second term in the square brackets of eq 6 is computed using eq 11 and eq 12.

$$(\partial/\partial P_{\mu\nu})\mathbb{Q} = \mathcal{B}^{-1}\,(\partial/\partial P_{\mu\nu})\mathbb{Q}^0 \tag{11}$$

$$[(\partial/\partial P_{\mu\nu})\mathbb{Q}^0]_i \approx f_\epsilon \Delta s_i(\partial/\partial n)V_{i_{\mu\nu}} \tag{12}$$

The only experimentally derived quantities that enter the theory are the radii of the atomic spheres. In order to avoid any subjective bias, standard van der Waals radii suggested by Bondi[27] are used.

All calculations were carried out using a modified version of MOPAC with the published AM1 and MNDO parameterizations.[23-25] There are still unresolved problems in the computation

---

(13) Cramer, C. J.; Truhlar, D. G. *J. Comput.-Aided Mol. Des.* In press.

(14) Cramer, C. J.; Truhlar, D. G. *J. Comput. Chem.* **1992**, *13*, 1089–1097.

(15) Miertuš, S.; Scrocco, E.; Tomasi, J. *Chem. Phys.* **1981**, *55*, 117–129.

(16) Bonaccorsi, B.; Cimiraglia, R.; Tomasi, J. *J. Comput. Chem.* **1983**, *4*, 567–577. Alagona, G.; Ghio, C.; Igual, J.; Tomasi, J. *J. Mol. Struct.* (*THEOCHEM*) **1990**, *204*, 253–283. Bonaccorsi, B.; Palla, P.; Tomasi, J. *J. Am. Chem. Soc.* **1984**, *106*, 1945–1950.

(17) Alagona, G.; Ghio, C.; Igual, J.; Tomasi, J. *J. Am. Chem. Soc.* **1989**, *111*, 3417–3421.

(18) Pascual-Ahuir, J. L.; Silla, E.; Tomasi, J.; Bonaccorsi, R. *J. Comput. Chem.* **1987**, *8*, 778–787.

(19) Miertuš, S.; Frecer, V.; Majekova, M. *J. Mol. Struct.* (*THEOCHEM*) **1988**, *179*, 353–366. Frecer, V.; Majekova, M.; Miertuš, S. *Ibid.* **1989**, *183*, 403–419.

(20) Hoshi, H.; Sakurai, M.; Inoue, Y.; Chûjô, R. *J. Chem. Phys.* **1987**, *87*, 1107–1115. Hoshi, H.; Sakurai, M.; Inoue, Y.; Chûjô, R. *J. Mol. Struct.* (*THEOCHEM*) **1988**, *180*, 267–281. Furuki, T.; Sakurai, M.; Inoue, Y.; Chûjô, R.; Harata, K. *Chem. Phys. Lett.* **1992**, *188*, 584–588.

(21) Wang, B.; Ford, G. P. *J. Chem. Phys.* **1991**, *97*, 4162–4169.

(22) Stewart, J. J. P. *QCPE Bull.* **1983**, *3*, 43.

(23) Dewar, M. J. S.; Zoebisch, E. G.; Healy, E. F.; Stewart, J. J. P. *J. Am. Chem. Soc.* **1985**, *107*, 3902–3909.

(24) Dewar, M. J. S.; Zoebisch, E. G. *J. Mol. Struct.* (*THEOCHEM*) **1988**, *180*, 1–21.

(25) Dewar, M. J. S.; Thiel, W. *J. Am. Chem. Soc.* **1977**, *99*, 4899–4907, 4907–4917. Dewar, M. J. S.; Rzepa, H. H. *J. Comput. Chem.* **1983**, *4*, 158–169.

(26) The form of the Schrödinger equation used here (eq 1) differs from the one used by the Tomasi and co-workers[15-18] by the factor of $^1/_2$ in the Hamiltonian. This is connected with the fact that eq 1 refers to the total energy of the solute–solvent system,[21] while the Hamiltonian in which the factor $^1/_2$ does not appear[15-18] refers specifically to the solute. In particular, the present Hamiltonian includes the self-repulsion energy within the solvent (resulting from its polarization by the solute). In the alternative philosophy, adopted by Tomasi and co-workers, the latter is not included in the Hamiltonian (and therefore the computation of the wave function) but is instead treated as a correction to the solute energy in the final computation of the hydration free energy (cf. eq 5 of ref 17).

(27) Bondi, A. *J. Phys. Chem.* **1964**, *68*, 441–451.

Table I. Comparison of the Computed Electrostatic Hydration Energies and the Experimental Total Hydration Energies of Neutral Molecules (kcal mol^{-1})

	ΔH_f (gas)		$\Delta G^{\circ\, g\rightarrow aq}$		
molecule	AM1	MNDO	AM1	MNDO	exptl[a]
CH_4	−8.7	−11.9	−0.1	−0.01	1.95
Me_3CH	−29.4	−26.8	−0.7	−0.01	2.29
MeCCH	43.4	41.4	−4.5	−2.0	−0.48
PhEt	8.6	40.5	−7.6	−1.0	−0.61
MeCl	−18.9	−22.5	−1.8	−2.9	−0.53
Me_2CHCl	−31.2	−32.1	−2.4	−3.0	−0.25
MeCN	19.3	19.2	−3.8	−2.6	−3.89
$MeNH_2$	−7.4	−7.5	−1.2	−0.6	−4.56[b]
Me_3N	−1.7	−2.8	−1.9	−1.2	−3.23
H_2O	−59.2	−60.9	−2.4	−1.6	−6.32[c]
MeOH	−57.0	−57.4	−2.4	−1.5	−5.07
Me_2CHOH	−69.5	−65.1	−2.7	−1.6	−4.75
Me_2O	−53.2	−51.2	−3.5	−1.9	−1.90
THF	−58.4	−59.3	−4.4	−2.2	−3.46
1,4-dioxan	−94.8	−87.6	−6.5	−4.3	−5.05
PhOMe	−15.8	−18.2	−8.4	−2.8	−1.04
MeCHO	−41.6	−42.3	−5.3	−3.6	−3.51
$Me_2C{=}O$	−49.2	−49.4	−5.6	−3.8	−3.81
cyclopentanone	−55.3	−57.0	−5.2	−3.1	−4.86[d]
$MeCO_2H$	−103.0	−101.1	−7.1	−5.8	−6.70
$MeCO_2Me$	−96.4	−93.7	−7.6	−5.8	−3.32
$MeCONH_2$	−50.7	−48.2	−9.5	−6.0	−9.7[e]
guanine	48.8	7.8	−22.2	−13.6	~−14[f]

[a] Data from ref 28. [b] Cabani, S.; Gianni, P.; Mollica, V.; Lepori, L. *J. Solution Chem.* **1981**, *10*, 563–595. [c] Value = $-RT \ln (c_l/c_g)$, where c_l is the concentration in 1 L of the liquid phase (=55.3 M) and c_g is the concentration in 1 L of the gas computed from the partial pressure of water (=23.76 mmHg) (*CRC Handbook of Chemistry and Physics*, 60th ed.; CRC Press: Boca Raton, FL, 1979). [d] Estimated value from additivity rules in ref 28. [e] R. Wolfenden, *J. Am. Chem. Soc.* **1976**, *98*, 1987–1988. [f] Estimated value for 9-methylguanine, see ref 30.

Table II. Comparison of the Computed Electrostatic Hydration Energies and the Experimental Hydration Energies of Cations (kcal mol^{-1})

	ΔH_f (gas)		$\Delta G^{\circ\, g\rightarrow aq}$		
molecule	AM1	MNDO	AM1	MNDO	exptl[a]
$MeNH_3^+$	148.7	161.7	−75.6	−76.5	−71.9
$Me_2NH_2^+$	149.2	162.3	−66.9	−68.6	−64.5
Me_3NH^+	152.0	167.2	−59.8	−60.4	−57.2
Me_2OH^+	136.6	138.8	−66.2	−68.2	−72.8
$Me_2C{=}OH^+$	125.5	127.3	−63.6	−65.4	−70.2
pyH^+	184.2	187.9	−60.6	−58.9	−56.7

[a] Data from ref 29 using $\Delta G^{\circ\, g\rightarrow aq}[NH_4^+] = -79.5$, see text.

Table III. Comparison of the Calculated Electrostatic Hydration Energies and the Experimental Hydration Energies of Anions (kcal mol^{-1})

	ΔH_f (gas)		$\Delta G^{\circ\, g\rightarrow aq}$		
molecule	AM1	MNDO	AM1	MNDO	exptl
HO^-	−14.1	−5.8	−106.0	−105.6	−107.5,[a] −106[b]
$N{\equiv}C^-$	44.0	55.3	−87.0	−87.6	−77[b]
$CH_3COCH_2^-$	−43.6	−43.0	−79.0	−74.2	−76,[c] −81[b]
CH_3O^-	−38.5	−39.7	−85.6	−82.1	−95[b,c]
PhO^-	−41.0	−42.2	−76.7	−67.1	−76,[c] −72[b]
$MeCO_2^-$	−115.4	−110.0	−83.3	−81.2	−82,[c] −77[b]
$PhCO_2^-$	−86.9	−82.0	−84.5	−78.2	−76[c,d]

[a] From data in refs 31 and 32. [b] Reference 33. [c] Reference 29. [d] Using $\Delta G^{\circ\, g\rightarrow aq}[PhCO_2H] \approx -7.7$, estimated from data in ref 28.

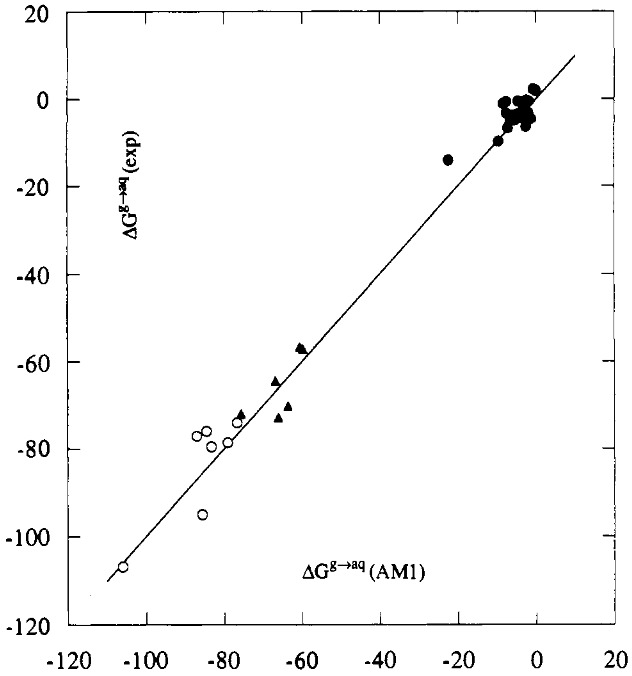

Figure 1. Comparison of calculated (AM1) and experimental hydration free energies. Neutral molecules ●; cations ▲; anions ○. Where more than one experimental value is given in Table III, the mean value was plotted.

of derivatives of the energy with respect to the internal coordinates when solvation effects are included. All computations of the latter kind were therefore carried out on geometries optimized in the gaseous state. While unfortunate, major errors from this source are not expected.

Results and Discussion

Hydration energies for a selection of neutral molecules, cations, and anions computed using both the AM1 and MNDO Hamiltonians are collected in Tables I–III together with the related experimental data for the same species. For the neutral compounds, these were mostly derived from data tabulated by Hine and Mookerjee[28] and refer to a standard state corresponding to the transfer of 1 mol of the gaseous solute to 1 L of aqueous solution. The experimental quantities for the ionic species are more troublesome. Taft has compiled extensive hydration free energy data for various oxygen and nitrogen protonated species relative to NH_4^+.[29] Unfortunately, the experimental value of the latter necessary to put these on an absolute scale is rather uncertain. We have recently argued in favor of a value of −79.5 kcal mol^{-1}, obtained[30] by revising the value of Klots[31] upward to bring it into line with the currently recommended proton hydration free energy.[32] Experimental anionic hydration free energies were obtained from the published[29] data for the exchange reaction $C_6H_5CH_2^- + HA \rightleftarrows C_6H_5CH_3 + A^-$ using hydration free energies of the neutral species from ref 28 and tied to the absolute scale using $\Delta G^{\circ\, g\rightarrow aq}[OH^-] = -107.5$ kcal mol^{-1}. The latter corresponds to the value given by Klots,[31] again after adjustments to the proton hydration free energy mentioned above.[32] Of the three classes of compounds, these hydration energies are the least certain. We have, therefore, also included analogous data tabulated by Pearson.[33] In some cases, those from the two sources differ by as much as 5 kcal mol^{-1}.

Precise comparison between the experimental and calculated quantities is complicated by the fact that the latter refer only to the electrostatic component of the total hydration energies. No explicit allowance is therefore made for specific hydrogen-bonding interactions. However, since the methodology is sensitive to the detailed charge distribution of the molecule or ion, these seem to be at least partially reflected in the computed hydration energies. Although there is no a priori reason to believe that they are, or can be, quantitatively included in this way, the results presented below suggest that in some cases such allowance is remarkably

---

(28) Hine, J.; Mookerjee, P. K. *J. Org. Chem.* **1975**, *40*, 292–298.

(29) Taft, R. W. *Prog. Phys. Org. Chem.* **1983**, *14*, 247–350.

(30) Ford, G. P.; Wang, B. *J. Comput. Chem.* **1992**, *13*, 229–239.

(31) Klots, C. E. *J. Phys. Chem.* **1981**, *85*, 3585–3588.

(32) After adjusting to the standard state used here, $\Delta G^{\circ\, g\rightarrow aq}[H^+] = -260.9$ kcal mol^{-1}, Trasatti, S. *Pure Appl. Chem.* **1986**, *58*, 955–966.

(33) Pearson, R. G. *J. Am. Chem. Soc.* **1986**, *108*, 6109–6114.

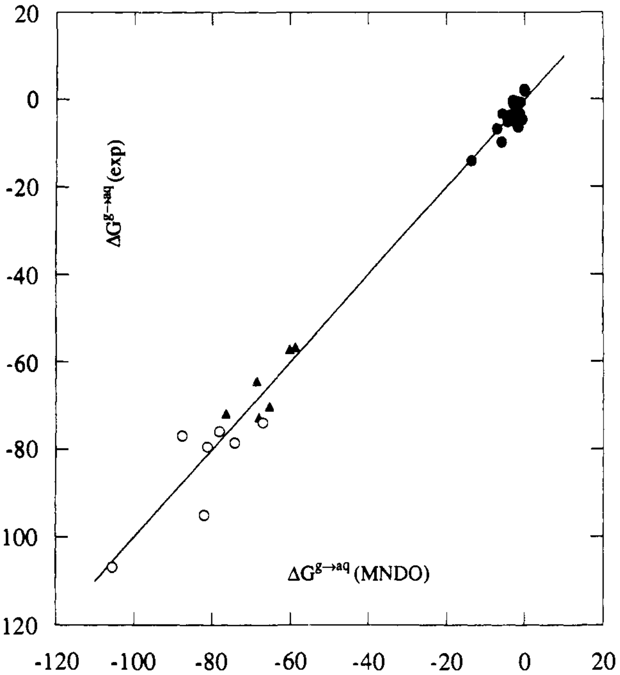

Figure 2. Comparison of calculated (MNDO) and experimental hydration free energies. Neutral molecules ●; cations ▲; anions ○. Where more than one experimental value is given in Table III, the mean value was plotted.

Table IV. Comparison of the AM1 Electrostatic Hydration Energies and the Experimental Total Hydration Energies of Ionic Hydrates (kcal mol^{-1})

molecule	ΔH_f (gas) AM1	$\Delta G^{\circ\, g\to aq}$ AM1	$\Delta G^{\circ\, g\to aq}$ exptl[a]
$Me_3NH^+\cdots OH_2$	80.8	−55.8	−53
$Me_2OH^+\cdots OH_2$	61.2	−59.9	−59
$Me_2C{=}OH^+\cdots OH_2$	52.0	−57.9	−60
$CH_3O^-\cdots OH_2$	−114.2	−78.2	−80
$CH_3CO_2^-\cdots OH_2$	−188.1	−78.1	−75, −70[b]

[a] Data for monohydrated ions calculated from hydration free energies of the uncomplexed ions (Tables II and III) and the gas-phase attachment energies,[39] cf. ref 30. [b] Using hydration free energy of $CH_3CO_2^-$ from ref 33.

Table V. Comparison of Calculated (AM1) Hydration Energies Obtained Here with Those Using a Multipolar Expansion within an Ellipsoidal Cavity

	method			method	
molecule	present work	multipole[a] expansion	molecule	present work	multipole[a] expansion
Me_3CH	−0.7	−0.2	$MeCONH_2$	−9.5	−11.2
Me_2CHCl	−2.4	−1.6	$MeNH_3^+$	−75.6	−76.2
Me_2CHOH	−2.7	−4.7	$Me_2NH_2^+$	−66.9	−68.4
$MeNH_2$	−1.2	−3.6	Me_3NH^+	−59.8	−59.2
$MeC{\equiv}N$	−3.8	−5.4	Me_2OH^+	−66.2	−69.1
$Me_2C{=}O$	−5.6	−7.3	$Me_2C{=}OH^+$	−63.6	−65.0
$MeCO_2Me$	−7.6	−7.9			

[a] Data from ref 30 and unpublished work by the present authors using the same methods.

complete. On the other hand, no accounting whatsoever is made for cavity forming and related "hydrophobic" contributions.

Despite the foregoing difficulties, it is clear that the overall correspondence between the computed and experimental hydration energies based on both the AM1 and MNDO Hamiltonians is quite close (Figures 1 and 2). Further, some of the most obvious discrepancies are, at least qualitatively, of just the kind expected to result from the approximations inherent in the model. For example, among the neutral molecules lacking significant lone-pair moments (alkanes, chloroalkane), the computed hydration energies are too negative by 1–3 kcal mol^{-1}, which is about the magnitude of the hydrophobic contribution ignored in the method.[12,34] On the other hand, the hydration energies of alcohols and amines are too positive. This is due in part to the use of predetermined atomic radii without regard to their environment, which results here in hydrogen radii for OH and NH groups that are too large.[35] However, the principal culprit is almost certainly the approximation inherent in eq 5, which eliminates the "lone pair" moments of the heteroatoms.

While the foregoing problems relate to the solvation model, the data in Table I reveal what appears to be a failure of the AM1 wave function itself. Thus, the computed hydration energies of the planar aromatic compounds are too negative by amounts that are far too large to be explicable in terms of the neglect of hydrophobic factors. This problem is not evident in the MNDO data and seems to be connected with the tendency of AM1 to exaggerate the polarities of bonds to hydrogen, especially those to unsaturated carbon atoms.[36]

Although the experimental data are rather less well established, similar comparisons for the ionic species provide very useful insights into the ability of the continuum model to reproduce experimental hydration energies of systems in which specific hydrogen-bonding interactions are expected. This is especially true for the conjugate acids in Table II which include highly polar NH and OH groups which interact strongly with the aqueous solvent.[29,37,38] In the absence of an explicit accounting for hydrogen-bonding interactions, a continuum-based computation would be expected to underestimate the hydration energies of these species. Remarkably, this is not universally the case. The AM1 and MNDO electrostatic hydration energies of the protonated primary, secondary, and tertiary amines are very similar to, and indeed slightly more negative than, the experimental data (Table II) by amounts consistent with the neglected hydrophobic components. The electrostatic model, therefore, appears to mimic the specific hydrogen-bonding interactions in these ions unexpectedly well. This seems to validate Cramer and Truhlar's at first sight rather questionable parameterization of an extended Born procedure using experimental data for both neutral molecules and protonated bases.[12-14] On the other hand, the ability of the method to account for the hydration energies of protonated oxygen bases is less complete. This is perhaps not unexpected. According to empirical estimates,[38] specific hydration effects contribute significantly more to the hydration energies for oxonium ions than they do for protonated amines. Some evidence for similar problems among the anionic species is suggested by the data in Table III, although the experimental data are too uncertain to draw firm conclusions here. If discrepancies between the computed and experimental hydration energies are indeed due to the neglect of specific hydrogen-bonding contributions, then these should be largely eliminated by comparing the experimental and computed data, not for the ions themselves, but for their hydrates. This is done for the AM1 data in Table IV (similar calculations using MNDO are not possible since the gas-phase clusters are unbound). Here, the relevant experimental quantities were obtained from a thermocycle involving the experimental gas-phase attachment energies[39] as described before.[30] As expected, the agreement between the experimental and theoretical quantities is essentially

---

(34) Still, W. C.; Tempczyk, A.; Hawley, R. C.; Hendrickson, T. *J. Am. Chem. Soc.* **1990**, *112*, 6127–6129.

(35) Reducing the radii of the hydrogen atoms in these environments naturally increases the computed hydration energies. However, from our preliminary investigation it is clear that such reductions alone, at least within sensible limits, are inadequate to correct the discrepancies in compounds of this kind.

(36) Besler, B. H.; Merz, K. M., Jr.; Kollman, P. A. *J. Comput. Chem.* **1990**, *11*, 431–439.

(37) Taft, R. W.; Wolf, J. F.; Beauchamp, J. L.; Scorrano, G.; Arnett, E. M. *J. Am. Chem. Soc.* **1978**, *100*, 1240–1249. Meot-Ner (Mautner), M. *J. Phys. Chem.* **1987**, *91*, 417–426.

(38) Ford, G. P.; Scribner, J. D. *J. Org. Chem.* **1983**, *48*, 2226–2233.

(39) Meot-Ner (Mautner), M. *J. Am. Chem. Soc.* **1984**, *106*, 1265–1272. Meot-Ner (Mautner), M.; Sieck, L. W. *J. Am. Chem. Soc.* **1986**, *108*, 7525–7529.

Table VI. AM1 and MNDO Data for Cytosine Tautomers (kcal mol^{-1})[a]

		cytosine tautomer		
	method	**1**	**2a**	**2b**
$\Delta G^{\circ}{}_{g\to aq}$	AM1	−18.6	−12.4	−12.1
$\Delta\Delta G^{\circ}{}_{g\to aq}$	AM1	0.0	6.2	6.5
$\Delta G^{\circ}{}_{g\to aq}$	MNDO	−11.9	−8.5	−8.4
$\Delta\Delta G^{\circ}{}_{g\to aq}$	MNDO	0.0	3.4	3.5

[a] $\Delta\Delta G^{\circ}{}_{g\to aq} = \Delta G^{\circ}{}_{g\to aq}(2) - \Delta G^{\circ}{}_{g\to aq}(1)$.

unchanged for Me_3NH^+ but undergoes substantial improvement for the oxonium ions, as well as for CH_3O^-.

Table V compares the AM1 hydration energies obtained using the present methodology with those given by the cavity model of Rinaldi and co-workers.[4] These results, based on the same wave function and geometries, were obtained using the GEOMOS program[40] with a multipolar description of the solute complete to the 2^6 order. While the underlying theories of the two methods are quite different, they both attempt to model the aqueous environment as a continuum within the SCRF formalism. Thus, differences in the predicted hydration energies should be limited to those arising from differences in the nature of the cavities used and the specific approximations inherent in each approach. As emphasized in the Introduction, a principal difficulty associated with the cavity model lies in the definition of the cavity itself. The data in Table V were mostly obtained in our earlier work,[30] in which the solutes were placed in ellipsoidal cavities, the dimensions and orientations of which were optimized in a procedure[30] based on the minimization of the classical interaction energy between the solute and a water-like probe. While it is certainly not true for all molecules, each of those in Table V is reasonably well represented by an ellipsoidal envelope. The effect of truncation of the multipolar expansion at the sixth order is not known. However, the method should be greatly superior to the frequently executed calculations based only on monopole and dipole terms. The principal deficiency of the present method almost certainly lies in the simplifications currently made in the integral calculations, which lead directly to the loss of many subleties of the three-dimensional electron distribution of the solute. This has already been mentioned in connection with the hydration energies of molecules, for which lone-pair moments are surely of importance, and accounts for the underestimation of these data for alcohols and amines with respect to both the experimental data and those computed in the multipolar expansion method. Nevertheless, the overall agreement between the two very different types of calculations is reassuringly close (the linear correlation coefficient between the two sets of hydration energies is 0.999).

We next turned to the examination of some reaction processes in aqueous solution. Cytosine derivatives substituted at the 1-nitrogen exist in two principal tautomeric forms, **1** and **2**, with

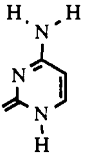

1

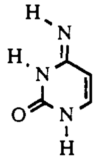

2a

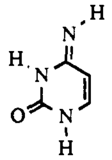

2b

both *Z* (**2a**) and *E* (**2b**) configurations possible for the latter. The computed absolute and relative hydration energies at the AM1 and MNDO levels are summarized in Table VI.[41] According to the free energy perturbation calculations of Kollman and co-workers,[42] the "normal" tautomer (**1**) is more strongly solvated than **2b** by 4.2 ± 0.1 kcal mol^{-1} (**2a** was not studied). MNDO gives a similar although slightly smaller value of 3.5 kcal mol^{-1}.

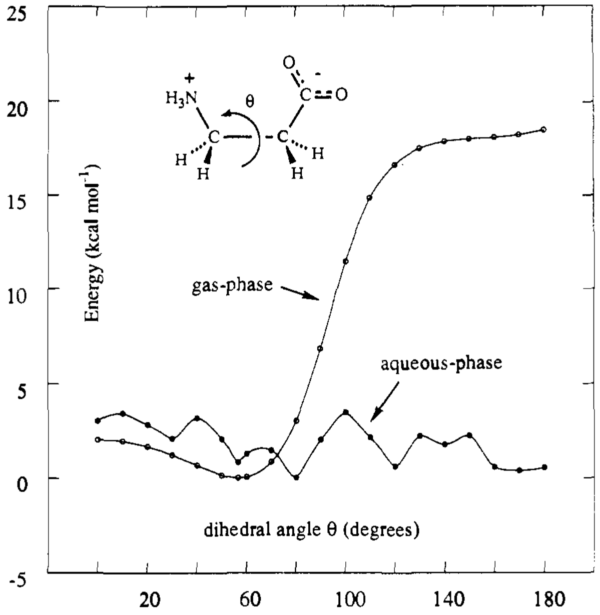

Figure 3. Computed (AM1) gaseous- and aqueous-phase energy profiles for rotation about the central C–C bond in *β*-alanine (**3**). The fully eclipsed and anti conformations correspond to $\theta = 0°$ and 180°, respectively.

AM1, which as described above overestimates the absolute hydration energies of aromatic molecules, also exaggerates the difference between the solvation energies of the alternative tautomers.

We next considered the AM1 energy profile for rotation about the central C–C bond in the zwitterionic molecule **3**. The solution

$$H_3N^+CH_2CH_2CO_2^-$$

3

conformations of the zwitterionic forms of α,ω-amino acids have been studied in detail.[43] While the anti conformer is highly destabilized in the gas phase,[44,45] in aqueous solution, conformations in which the charged groups are either proximal or distal are approximately equally populated.[43] As in the HF/4-31G molecular orbital calculations of Ramek, the eclipsed conformation was not a local minimum with respect to reversion to the non-zwitterionic form.[44] In order to obtain the gas-phase profile, it was therefore necessary to artificially constrain the N–H bond lengths to the distances computed for the anti conformer (1.0 Å) throughout the rotational pathway. All other variables were optimized as the NCCC dihedral angle θ was sequentially increased in steps of 10°. The energy of the resulting geometry at each point was then recomputed in the simulated aqueous environment. The results are summarized in Figure 3. The minimum on the gas-phase profile corresponds to a gauche-like geometry with $\theta = 44°$ and rises to a maximum as θ approaches 180°. The solution-phase profile is quite different. While there is considerable "noise" in the computed profile, all points fall within ca. 3.5 kcal mol^{-1} of one another with broad minima corresponding to gauche and anti geometries of about equal energy.

The prototypical S_N1 and S_N2 reactions were examined as examples of processes involving the making and breaking of chemical bonds, where the gaseous- and aqueous-phase behavior is expected to be quite different. The identity S_N2 reaction shown in eq 13 has been studied in detail by Jorgensen and co-workers

$$Cl^- + CH_3Cl \rightarrow ClCH_3 + Cl^- \qquad (13)$$

using a 6-31G(d) basis set ab initio calculation in conjunction with

---

(40) Rinaldi, D.; Hoggan, P. E.; Cartier, A. *QCPE Bull.* **1989**, *9*, 128–192.

(41) For a discussion of the gas-phase tautomerization energies using AM1 and MNDO, see: Fabian, W. M. F. *J. Comput. Chem.* **1991**, *12*, 17–35.

(42) Cieplak, P.; Bash, P.; Singh, U. C.; Kollman, P. A. *J. Am. Chem. Soc.* **1987**, *109*, 6283–6289.

(43) Abraham, R. J.; Loftus, P.; Thomas, W. A. *Tetrahedron* **1977**, *33*, 1227–1234. Kirchnerova, J.; Farrell, P. G.; Edward, J. T. *J. Phys. Chem.* **1976**, *80*, 1974–1980.

(44) Ramek, M. *J. Mol. Struct.* (*THEOCHEM*) **1990**, *67*, 301–355.

(45) Gresh, N.; Pullman, A.; Claverie, P. *Theor. Chim. Acta* **1985**, *67*, 11–32.

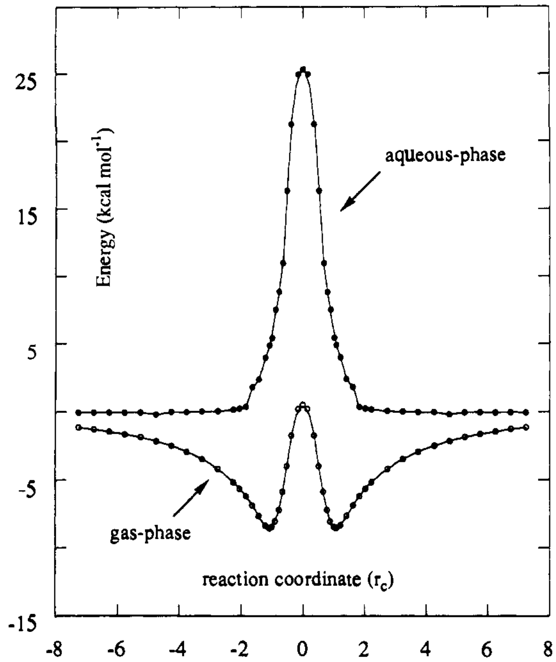

Figure 4. Computed (AM1) gaseous- and aqueous-phase energy profiles for the S_N2 reaction of Cl^- and CH_3Cl (eq 13). The reaction coordinate (Å) $r_c = r_{C-Cl} - r_{C-Cl'}$.

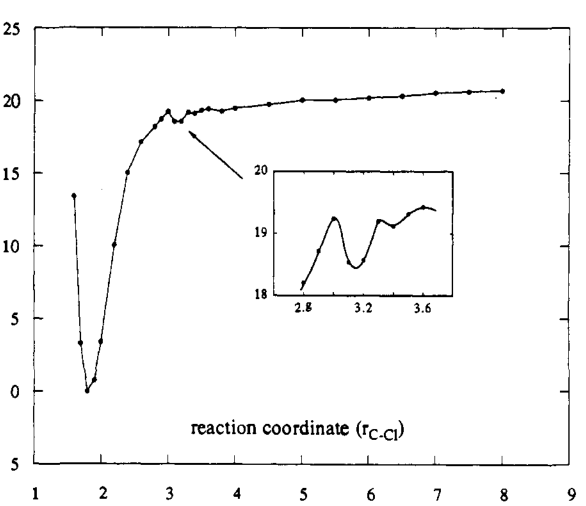

Figure 5. Computed (AM1) aqueous-phase energy profile for the S_N1 heterolysis of the C–Cl bond in *t*-BuCl.

a Monte Carlo simulation of the aqueous environment.[46] For comparison with the latter workers, we define a reaction coordinate r_c equal to $r_{CCl} - r_{CCl'}$. The AM1 reaction path was first computed in the gas phase by minimizing the geometry for a range of values of r_c within the constraints of C_{3v} symmetry. The energy of each point was then recomputed in the simulated aqueous environment. The computed gaseous- and condensed-phase reaction profiles are shown in Figure 4. The former has the familiar[47] double-well shape in which the central maximum lies 9.1 kcal mol^{-1} above the flanking ion–dipole complexes, which themselves lie 8.6 kcal mol^{-1} below the reactants. Identical results were obtained earlier by Dewar and Zoebisch[24] and are in very satisfactory agreement with the corresponding experimental values of 11.6 ± 1.8[48] and 8.6[49] kcal mol^{-1}, respectively. As did Jorgensen's Monte Carlo simulations,[46] the reaction profile becomes unimodal in the aqueous phase. The maximum is computed to be 25.4 kcal mol^{-1} above the energy of the isolated reactants, which compares very favorably with the experimental activation barrier of 26.5 kcal mol^{-1}.[50] Similar results were obtained using MNDO, where the barrier in the aqueous phase was computed to be 28.6 kcal mol^{-1}. Like the far more sophisticated Monte Carlo calculations, these results indicate that most of the activation barrier in the aqueous phase arises through the desolvation of the transition state. Interestingly, an MNDO study of this system by Kikuchi and co-workers using an extended Born model grossly underestimated this effect, resulting in an aqueous-phase barrier of only 13 kcal mol^{-1}.[10]

According to the current view,[51] elongation of the bond to the leaving group of S_N1 substrates leads ultimately to the fully dissociated ions via a "tight" ion pair and then a "solvent-separated" ion pair. This is illustrated using the usual symbolism for *t*-BuCl in eq 14. The gas-phase reaction profile was computed

$$\underset{}{(CH_3)_3C\text{–}Cl} \rightleftarrows \underset{\text{tight ion pair}}{(CH_3)_3C^+Cl^-} \rightleftarrows \underset{\text{solvent-separated ion pair}}{(CH_3)_3C^+||Cl^-} \rightleftarrows (CH_3)_3C^+ + Cl^- \quad (14)$$

by minimizing the AM1 (UHF) heat of formation of the system for successively longer values of the CCl bond within the constraints of C_3 symmetry. Each point was then recomputed in the simulated aqueous environment as before. The resulting reaction profile is shown in Figure 5. Since the lowest-energy gas-phase process is a homolytic one, the computed geometries refer to those of the incipient *t*-Bu radical rather than the cation. However, this error, which is greatest at larger separations, amounts to only ca. 1 kcal mol^{-1} for $r_{CCl} \geq 8$ Å. The fully dissociated reactants (geometry optimized for *t*-Bu$^+$) are computed to lie 20.5 kcal mol^{-1} above the reactants. This is very close to the activation free energy of 19.6 kcal mol^{-1} for the solvolysis of an aqueous solution measured by Winstein and Fainberg.[52] The computed reaction pathway (Figure 3) shows a maximum at $r_{CCl} = 3.0$ Å that is 18.1 kcal mol^{-1} above the reactants, followed by a rather shallow (ca. 0.9 kcal mol^{-1}) minimum at $r_{CCl} = 3.3$ Å. Given the obvious crudeness of the model, the appearance of such a minimum in the region close to that expected[53] for the tight ion pair is rather interesting. On the other hand, a second minimum corresponding to a solvent-separated ion pair is not evident, nor would one be expected in a continuum-based theory. As indicated by the Monte Carlo simulation of Jorgensen and co-workers,[53] the existence of such species is strongly dependent on specific interactions with bridging water molecules. Nevertheless, the prediction of about the right energy of the separated ions, together with the existence of a tight ion-pair-like species, seems an unexpectedly gratifying result.

Conclusion

The electrostatic hydration energies of a variety of neutral molecules and ions, together with the energetics of several aqueous-phase reaction processes, have been computed within the framework of semiempirical molecular orbital theory using a new formulation of an approach originally suggested by Tomasi and co-workers. No attempt has been made to optimize the performance of the model via the introduction of disposable parameters. While the development of the theory is at an early stage, the present results demonstrate that already it provides a qualitatively and in some cases a quantitatively correct description of each of the reaction processes considered. A broad correspondence between the experimental absolute hydration energies of both neutral and ionic species and the computed hydration energies

---

(46) Chandrasekhar, J.; Smith, S. F.; Jorgensen, W. L. *J. Am. Chem. Soc.* **1985**, *107*, 154–163.

(47) Olmstead, W. N.; Brauman, J. I. *J. Am. Chem. Soc.* **1977**, *99*, 4219–4228.

(48) Recomputed by Chandrasekhar et al.[46] from data in Brauman, J. I.; Olmstead, W. N.; Lieder, C. A. *J. Am. Chem. Soc.* **1974**, *96*, 4030–4031.

(49) Dougherty, R. C.; Roberts, J. D. *Org. Mass Spectrom.* **1974**, *8*, 81–83.

(50) Albery, W. J.; Kreevoy, M. M. *Adv. Phys. Org. Chem.* **1978**, *16*, 87–157.

(51) Lowry, T. H.; Richardson, K. S. *Mechanism and Theory in Organic Chemistry*; 3rd ed.; Harper and Row: New York, 1987; pp 335–349.

(52) Winstein, S.; Fainberg, A. H. *J. Am. Chem. Soc.* **1957**, *79*, 5937–5950.

(53) Jorgensen, W. L.; Buckner, J. K.; Huston, S. E.; Rossky, P. J. *J. Am. Chem. Soc.* **1987**, *109*, 1891–1899.

J. Am. Chem. Soc. **1992**, *114*, 10569–10572

exists. Moreover, differences that do occur can be reasonably attributed to factors inherent in the continuum model or to approximations made in the present formalism and conveniently point the way to possible future improvements. In general, the MNDO results seem to be slightly superior to those obtained using AM1, which is probably a result of the better description of the electron distribution afforded by the older method. In this respect, AM1 fares rather poorly for neutral aromatic systems in which the predicted hydration energies are too negative.

Remarkably, the hydration energies of protonated amines are adequately treated by the present continuum method without the explicit inclusion of water molecules coordinated to the polar N–H bonds. This is not wholly true, however, for the hydration of the even more polarized conjugate acids of the oxygen bases.

Where comparisons were possible, the computed hydration energies were quite similar to those obtained using Rinaldi's multipolar expansion technique for a solute within an optimized ellipsoidal cavity. However, in contrast to the latter method, which critically depends on the ability to fit the solute within a cavity of specified shape, the present method is applicable to molecules, ions, and reacting systems of arbitrary shape.

Acknowledgment. We thank the Robert A. Welch Foundation for financial support of this work through grant N-1080.

Macrocyclic, Square Planar, Tetraalkynyl Tetraiodonium Salts: Structures, Stabilities, and Vibrational Frequencies via ab Initio Calculations

Alexander I. Boldyrev, Viktor V. Zhdankin, Jack Simons,* and Peter J. Stang*

Contribution from the Department of Chemistry, The University of Utah,
Salt Lake City, Utah 84112. *Received June 30, 1992*

Abstract: The geometries and stabilities of HCCH, ICCH, ICCI, IF_3, IF_2CCH, $IF(CCH)_2$, $I(CCH)_3$, $I_4(CC)_4{}^{4+}$, and four isomers of $I_4(CC)_4F_4$ were calculated at the ab initio HF/LANL1DZ level. Final geometries were used for electron correlation calculations at the MP4/LANL1DZ level. The results of the calculations demonstrate considerable stability and suggest square planar structures for the macrocyclic tetraalkynyl tetraiodonium compounds. The tetracation $I_4C_8{}^{4+}$ is predicted to exist as a single isomer due to a pseudotetrahedral 8-I-2 configuration and to have a structure with only negligible deviations from a perfect square. In contrast, the neutral $I_4C_8F_4$ species can exist as four different isomers as a consequence of the trigonal bipyramidal 10-I-3 configuration. These isomers have distinctly different geometries and energies due to the relative positions of the axial and equatorial C–I bonds. Macrocycles **16–19** have ring strain energy due to the existence of four unfavorable axial I–C bonds in each of the isomers. However, the calculated ring strain energy for the most stable isomer **16** is only 27 kcal/mol.

Introduction

There is considerable current interest in multicoordinate, polyvalent (hypervalent) main-group species.[1] Among the oldest, most interesting, and most extensively investigated polyvalent main-group compounds are those of iodine.[2] Multicoordinated iodine compounds with at least one organic ligand have been known since the discovery of $PhICl_2$ by Willgerodt in 1886.[3] In the intervening 100 years, thousands of polycoordinated iodine compounds have been reported, the most common class being the diaryliodonium salts. The latest members of this family, the alkynyl(phenyl)iodonium species,[4] have become valuable reagents for the ready preparation of diverse functionalized acetylenes[5] and other useful transformations.[6,7] Recently several new structural types of alkynyliodonium salts have been synthesized, such as bis(phenyliodonium)acetylene **1**,[7a] dialkynyliodonium salts **2**,[8] and *p*-phenylenebis(alkynyliodonium) triflate **3**.[9] However, iodonium salts with three or more iodonium and alkynyl or aryl moieties in the molecule are still unknown.

The unique T-shaped geometry of iodine(III) compounds described as 10-I-3 (for neutral) or 8-I-2 (for monocationic) species

---

(1) Inter Alia: Oae, S.; Uchida, Y. *Acc. Chem. Res.* **1991**, *24*, 202. Martin, J. C. *Science (Washington, DC)* **1983**, *221*, 509. Bettermann, G.; Arduengo, A. J., III *J. Am. Chem. Soc.* **1988**, *110*, 877. Arduengo, A. J., III; Dixon, D. A.; Roe, D. C.; Kline, M. *J. Am. Chem. Soc.* **1988**, *110*, 4437. Brel', V. K.; Gakh, A. A.; Zhdankin, V. V.; Zefirov, N. S.; Koz'min, A. S.; Korkin, A. A.; Kutateladze, T. G.; Caple, R.; Lermontov, S. A.; Plokhikh, I. G.; Safronov, S. O.; Stang, P. J.; Chovnikova, N. G. *Dokl. Akad. Nauk SSSR* **1990**, *313*, 1131.

(2) (a) Varvoglis, A. *The Organic Chemistry of Polycoordinated Iodine*; VCH Publishers, Inc.: New York, 1992. (b) Reviews: Moriarty, R. M.; Vaid, R. K.; Koser, G. F. *Synlett* **1990**, 365. Moriarty, R. M.; Vaid, R. K. *Synthesis* **1990**, 431. Merkushev, E. B. *Russ. Chem. Rev.* **1987**, *56*, 826. Moriarty, R. M.; Prakash, O. *Acc. Chem. Res.* **1986**, *19*, 244. Ochiai, M.; Nagao, Y. *Kyokai Yuki Gosie* Kagaku Kyeokaishi **1986**, *44*, 660. Varvoglis, A. *Synthesis* **1984**, 709. Koser, G. F. In *The Chemistry of Functional Groups, Suppl. D*; Patai, S., Rappoport, Z., Eds; Wiley-Interscience: New York, 1983; Chapters 18 and 25, pp 721–811 and 1265–1351. Umemoto, T. *Kyokai Yuki Gosie Kagaku Kyeokaishi* **1983**, *41*, 251. Varvoglis, A. *Chem. Soc. Rev.* **1982**, *10*, 377.

(3) Willgerodt, C. *J. Pract. Chem.* **1886**, *33*, 155.

(4) Review: Stang, P. J. *Angew. Chem., Int. Ed. Engl.* **1992**, *31*, 274.

(5) Review: Stang, P. J. *Acc. Chem. Res.* **1991**, *24*, 304.

(6) Lodaya, J. S.; Koser, G. F. *J. Org. Chem.* **1990**, *55*, 1513. Margida, A. J.; Koser, G. F. *Ibid.* **1984**, *49*, 4707. Carman, C. S.; Koser, G. F. *Ibid.* **1983**, *48*, 2534. Ochiai, M.; Ho, T.; Takaoka, Y.; Masaki, Y.; Kunishima, M.; Tani, S.; Nagao, Y. *J. Chem. Soc., Chem. Commun.* **1990**, 118. Ochiai, M.; Kunishima, M.; Nagao, Y.; Fuji, K.; Shiro, M.; Fujita, E. *J. Am. Chem. Soc.* **1986**, *108*, 8281. Ochiai, M.; Kunishima, M.; Sumi, K.; Nagao, Y.; Fujita, E.; Arimoto, M.; Yamaguchi, H. *Tetrahedron Lett.* **1985**, 4501.

(7) (a) Stang, P. J.; Zhdankin, V. V. *J. Am. Chem. Soc.* **1990**, *112*, 6437. Stang, P. J.; Zhdankin, V. V. *Ibid.* **1991**, *113*, 4571. (b) Bachi, M. D.; Bar-Ner, N.; Crittell, C. M.; Stang, P. J.; Williamson, B. L. *J. Org. Chem.* **1991**, *56*, 3912. Stang, P. J.; Williamson, B. L.; Zhdankin, V. V. *J. Am. Chem. Soc.* **1991**, *113*, 5870. Stang, P. J.; Boehshar, M.; Lin, J. *Ibid.* **1986**, *108*, 7832. Stang, P. J.; Kitamura, T. *Ibid.* **1987**, *109*, 7561. Stang, P. J.; Boehshar, M.; Wingert, H.; Kitamura, T. *Ibid.* **1988**, *110*, 3272. Stang, P. J.; Kitamura, T.; Boehshar, M.; Wingert, H. *Ibid.* **1989**, *111*, 2225. Stang, P. J.; Kitamura, T.; Arif, A. M.; Karny, M.; Apeloig, Y. *Ibid.* **1990**, *112*, 374.

(8) Stang, P. J.; Zhdankin, V. V.; Arif, A. M. *J. Am. Chem. Soc.* **1991**, *113*, 8997.

(9) Stang, P. J.; Zhdankin, V. V.; Arif, A. M. *Mendeleev Commun.*, in press.

0002-7863/92/1514-10569$03.00/0